Steering Through Sequential Linear Path Segments

Shota Yamanaka
Meiji University and JSPS
Nakano, Tokyo, Japan
stymnk@meiji.ac.jp

Wolfgang Stuerzlinger
Simon Fraser University
Vancouver, Canada
w.s@sfu.ca

Homei Miyashita
Meiji University
Nakano, Tokyo, Japan
homei@homei.com

ABSTRACT
The steering law models human motor performance and has been verified to hold for a single linear and/or circular path. Some extensions investigated steering around corners. Yet, little is known about human performance in navigating joined linear paths, i.e., successions of path segments with different widths. Such operations appear in graphical user interface tasks, including lasso operations in illustration software. In this work, we conducted several experiments involving joined paths. The results show that users significantly changed their behavior, and that this strategy change can be predicted beforehand. A simple model summing the two indexes of difficulty (*ID*s) for each path predicts movement time well, but more sophisticated models were also evaluated. The best model in terms of both of R^2 and *AIC* values includes the *ID* of the crossing operation to enter the second path.

Author Keywords
Steering law; graphical user interfaces; pointing; human performance; modeling; motor control.

ACM Classification Keywords
H.5.2. [Information interfaces and presentation]: User Interfaces - Input devices and strategies.

INTRODUCTION
The steering law was derived to model complicated tasks, such as writing a character, drawing a line, and navigating a path [1]. As one of the more robust models for human motor performance, the steering law has been verified to hold with various types of computer input devices [2, 25], various conditions such as 3D operations [7, 18] and even virtual reality car driving [31].

One goal of our work is to test the generality of the steering law. For example, it is interesting to see if it holds across different age groups [23] or to study the effects of the dominant hand [15]. In this paper, we investigate how well the steering law predicts sequences of path segments, i.e., joined paths. Except for a few studies, previous work usually conducted user experiments with a single linear and/or a circular tunnel. The only exploration beyond this focused on path segments joined at a corner. We could not find any study focusing on the application of the steering law for collinear paths with different widths. While navigating through paths that change width is an operation that occurs in graphical user interface (GUI) applications, no one has investigated how well the steering law predicts performance for such tasks.

CHI 2017, May 06-11, 2017, Denver, CO, USA
ACM 978-1-4503-4655-9/17/05.
http://dx.doi.org/10.1145/3025453.3025836

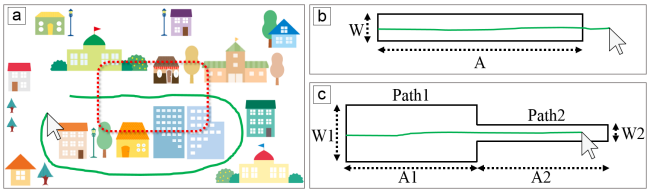

Figure 1. (a) A lasso operation (shown) as a green line. The part of the stroke highlighted in red traverses a tunnel with changing width (wide-to-narrow). (b) The steering law models strokes through a constant-width path. (c) Our work investigates steering through joined linear path segments with different widths, such as a wide-to-narrow path.

A more general form of a steering task is selecting objects in a drawing application through a lasso operation as shown in Figure 1a. When a user lassoes several objects, s/he must perform a sequence of steering operations through paths of varying widths and corners. Most previous literature on the steering law has focused on navigation through a single path segment, as shown in Figure 1b. User behaviors and strategies for navigation through more than one path segment (apart from corners) have not been analyzed in detail. As a first step towards a more general form of the steering law, we conduct several experiments for steering tasks involving two joined linear path segments (Figure 1c). The contributions of our work are as follows:

1) Based on a speed profile analysis of cursor trajectories, we identify that users change their movement strategies (a) in the presence of a path joint and (b) based on the width difference between two path segments.

2) We observed high fitness values in our experiments for a simple model that sums the two indexes of difficulty (*ID*s) for each segment to model the movement time (*MT*) for the entire path. Yet, taking the crossing operation to enter the second path segment (path2) into account improves the model fitness in both terms of R^2 and Akaike information criterion (*AIC*) values.

3) We also show that even when the two path segments have different lengths, the structure of the steering law automatically balances the weights for each segment on the entire *ID*.

RELATED WORK

While we introduced a lasso operation as an example of various types of stroking motions, in this paper we focus only on steering through two joined linear path segments. In this section and afterwards, *a*, *b*, *c*, and *d* in equations are empirically determined constants.

Steering Law Model

Laws of steering have been proposed by Rashevsky [20, 21] for car driving and Drury [11] for pen drawing. For GUI operations, Accot and Zhai represents a relationship between the movement time *MT* required to traverse a path with length *A* and width *W* [1]:

$$MT = a + b\frac{A}{W} \quad (1)$$

and *A*/*W* is also known as the index of difficulty (*ID*). This relationship was first confirmed using an indirect-input pen tablet [1] and subsequently for other computer input devices [2, 25]. Changes of the motor scale [3], start position [32], temporal constraint (time limit) [33], and path angle [27] were also tested. 3D manipulations [7, 18] and car driving [31] follow the steering law too.

Accot and Zhai also proposed that the average cursor speed *v* in the path linearly increases as its width increases [1]:

$$v = a + bW \quad (2)$$

where the *v* is *A*/*MT*.

A circular path with radius *r* can be modeled by replacing *A* with $2\pi r$ in Equation 1 [2, 3]. Models for linearly-narrowing paths [1], widening spiral paths [1], and the *MT* difference between linearly-narrowing and widening paths [30] have been presented. In this paper, we investigate only constant-width linear path segments.

Other Models for Steering Tasks

Modeling Steering Tasks with Pointing

When a user selects an item in cascading menus, s/he has to move the cursor within the boundaries and then click the intended item. This is called a targeted steering motion [9, 17, 24]. We discuss three models for such motions in detail, because we will later derive new models for joined paths from them in the discussion.

For pointing tasks, selecting a target of size *S,* which lies a distance *A* away, requires a movement time *MT*:

$$MT = a + b\log_2\left(\frac{A}{S} + 1\right) \quad (3)$$

and $\log_2(A/S + 1)$ is also called the *ID* of Fitts' law [12]. Dennerlein et al. proposed a model for targeted steering tasks with separated terms for the *ID* of the steering (ID_S) and pointing (ID_P) components [9]:

$$MT = a + bID_S + cID_P \quad (4)$$

Their results showed good fits with $R^2 \geq 0.98$. Kulikov and Stuerzlinger proposed a simpler model which sums ID_S and ID_P directly [17]:

$$MT = a + b(ID_S + ID_P) \quad (5)$$

This model was created to reduce the number of parameters in Dennerlein's model. Even for a model with few parameters, any extra free parameter naturally increases correlation but introduces overfitting [8, 17, 26], resulting in potentially inaccurate predictions of *MT*.

Senanayake et al. showed that ID_S and ID_P affect the total *MT* differently and thus simple sum of two *ID*s in Dennerlein's and Kulikov's methods cannot model more general path/target parameters [24]. They then proposed a model which separates the steering and the pointing phases, and which weighs *ID*s on the entire *MT*. In this model, a user is predicted to move the cursor without hitting the boundaries of the path for a distance of $(A - nW)$ at first, and then directly points to the final target, which lies a distance of $(nW + S/2)$ away, as illustrated in Figure 2:

$$MT = a + b\left(\frac{A - nW}{W}\right) + c\log_2\left(\frac{2(nW + S/2)}{S}\right) \quad (6)$$

In their results, $n = 5$ was an appropriate choice, based on Thibbotuwawa et al. [28] results. In Thibbotuwawa et al.'s work, they tested various combinations of *A* and *W* values, and confirmed that users do not need to perform the closed-loop steering phase when *A*/*W* is less than 5 [28]. Based on this observation, Equation 6 was derived, which models that users switch to target pointing at a distance of $5 \times W$ from the end. The *ID* for the pointing phase in Senanayake's model is based on a different formulation of Fitts' law:

$$MT = a + b\log_2\left(\frac{2(A + S/2)}{S}\right) \quad (7)$$

Senanayake et al. found that Equation 6 models targeted steering tasks better than Dennerlein's and Kulikov's work.

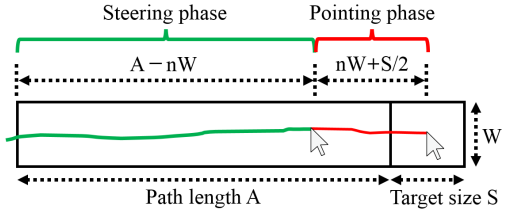

Figure 2. Two-phase model for targeted steering motion by Senanayake et al. [24].

Modeling Steering Tasks with Steering

Pastel found that when navigating a path with a corner in the middle, users steered in the first path segment, then stopped at the corner, and then steered again in the second

path segment [19]. Hence, passing through a tunnel whose center bends at a certain angle (45°, 90°, and 135°) can be predicted to require the time *MT*:

$$MT = a + bID_S + cID_P \quad (8)$$

where ID_P uses $A/2$ for the target distance. Pastel's experiment did not include conditions where the two path segments had different widths. In addition, this work did not verify model generality for the case of angle = 0°. We assume that a path with no bending (a 0°-corner) does not follow Pastel's model because users will not perform a stopping operation during their traversal of such a path.

Bateman et al. conducted steering law experiments in a racing video game [5]. The racing courses included three straight tracks connected by two 90° corners. Although they were aware of Zhai et al.'s driving experiments [31], they unfortunately did not show or discuss the fit of the steering law for their data.

In summary, navigating two linear path segments with different widths connected in a straight line (i.e., at 0° bend) cannot be directly expressed by previous models. The simplest way involving the least additional parameters would be to add the *ID* of the first (ID_1) and the second path segment (ID_2), similar to Kulikov's method:

$$MT = a + bID_{2SS} \quad (9)$$

$$ID_{2SS} = ID_1 + ID_2 \quad (10)$$

We call this the ID_{2SS} model, as it includes two free parameters for a combination of a steering and a steering task. This model can also be derived from the global form of the steering law [1]:

$$MT = a + b\int_0^A \frac{dx}{W(x)} \quad (11)$$

where A is the total path length, x is a position in the path, and $W(x)$ is the path width at x. According to this global law, the total *ID* of joined path segments is the sum of each *ID* of all the paths. If the ID_{2SS} model does not fit to the experimental data, we have to consider other models or additional free parameters. The comparison with other possible models will be discussed in *Overall Discussion*.

We assume that users' strategies could be different from that in a single path segment. E.g., with only a single path segment, the speed in the tunnel is expected to be constant per the steering law. The instantaneous speed v in a path is then determined by the path width W, as follows [1]:

$$v = \frac{W}{\tau} \quad (12)$$

where τ is the empirically determined time constant. On the other hand, if two path segments are joined, where the first path segment (path1) width W_1 is 50 pixels and the second (path2) width W_2 is 25 pixels (*narrowing* condition), a user has to decelerate in advance of the joint because the speed in path1 is faster than that of path2 according to Equation 12. The opposite condition (*widening*) might show different characteristics than *narrowing*. This asymmetric behavior cannot be predicted through the original steering law. Thus, the relationship of *MT* and *ID* might not hold for joined path segments with different widths. To address this potential shortcoming, we present here several experiments and, based on the results, discuss suitable steering models.

BASELINE EXPERIMENT 1: LINEAR PATH NAVIGATION

To establish a *baseline* for later comparisons of user strategies and behaviors, we first conducted a traditional steering law experiment involving a single linear path.

Apparatus

The PC was a Sony Vaio Z (Intel Core i7-5557U, 3.1 GHz; Intel Iris 6100; 16 GB; Windows 10). The input device and display was a Wacom Cintiq 27 QHD Touch DTK-2700/K0 (27" diagonal, 2560 × 1440 resolution, 596.7 × 335.6 mm active input area, 4.29 pixels/mm). The experimental system implemented with Hot Soup Processor 3.4 used full-screen mode. The system reads and processes input at approximately 125 times per second. The pen tablet was positioned on a table in "stand" mode (20 degrees, Figure 3). All participants wore a cotton artist glove to reduce friction. Participants were informed that their palms could touch the surface, as we had disabled finger touch sensing.

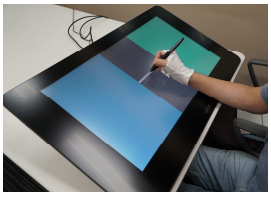

Figure 3. Experimental setting.

Participants

Thirteen volunteers participated in the experiment, of which three were female and ten male. The average age was 21.9 years (*SD* = 2.15). All participants had normal or corrected-to-normal vision and were right-handed. Three participants had 1 to 7 years of experience with using a stylus habitually.

Task

We reused the color scheme from previous work for the task areas: a blue starting area, a white path, and a green end area [16, 30]. The participants made a stroke within the white path as quickly and accurately as possible. A crosshair cursor left a trace from the moment of pen contact until lift-off. A bell sound was made when the cursor crossed the end line. A beep sounded when the cursor went over the path constraint. Then the participant had to retry the same task again. Going across the boundaries was counted as a steering error [3, 30], but lifting the pen tip during a trial was not considered an error. Still, if a user lifted the pen tip, the trial was suspended, and the participant had to redo the task again. Re-starting within a path or hovering was not permitted.

Design and Procedure

Two movement distances (A = 480 and 640 pixels, or 112 and 149 mm respectively) and four path widths (W = 15, 23, 33, and 45 pixels, or 3.50, 5.36, 7.69, and 10.5 mm respectively) were tested. The total number of combinations

of the parameters was 2(A) × 4(W) = 8. *ID*s ranged from 10.7 to 42.7 bits. One *block* consists of a random order of the 8 conditions. Participants first performed one practice block, and then ten blocks for data collection. Movement direction was always to the right. The recorded data for the actual tasks were 8 conditions × 10 blocks × 13 participants = 1040 trials. Participants took 6 to 7 minutes from the instructions to the completion of all tasks.

Results

After excluding lifting-pen instances (six trials), the total number of trials was 1079, with 39 steering errors (3.61%). Following previous work [1, 2, 3, 3029], we analyzed only error-free trials via repeated-measures ANOVA with a Bonferroni post hoc test. The speed profiles for experiment 1 will be analyzed with the results of experiment 2 later.

Movement Time MT

Figure 4a-c show the average *MT*. We observed main effects for A ($F_{1, 12}$ = 87.607, p < .001) and W ($F_{3, 36}$ = 48.130, p < .001). The post hoc test shows that navigation time increases as A increases (p < .001) and W decreases (p < .001 for all W pairs). We also observed a significant interaction of A × W ($F_{3, 36}$ = 33.095, p < .001); the *MT* difference between two A values decreases as W increases (Figure 4c). These tendencies are consistent with previous steering law studies with a stylus.

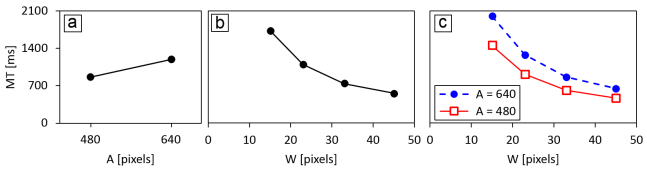

Figure 4. *MT* for (a) *A*, (b) *W*, and (c) *A* × *W* values.

Errors

We observed main effects for A ($F_{1, 12}$ = 10.749, p < .01) and W ($F_{3, 36}$ = 9.768, p < .001). We also observed a significant interaction of A × W ($F_{3, 36}$ = 9.141, p < .001). Averaged error rates were 1.52 and 5.63% for A = 480 and 640 pixels; 4.24, 2.80, 0.192, and 0% for W = 15, 23, 33, and 45 pixels, respectively.

Model Fitting

Figure 5a and b show that steering law held with excellent fits of R^2 > 0.99 for *MT* (Equation 1) and v (Equation 2) forms using eight A × W data points. This means that the experimental conditions of A and W values, and device, were all suitable for steering law tasks.

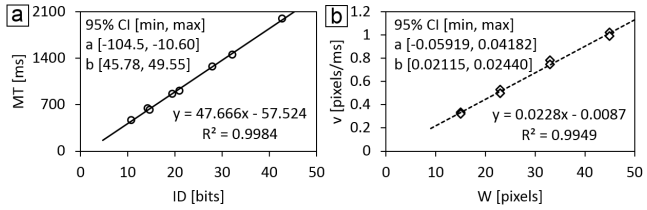

Figure 5. Steering law fitness with (a) *MT* and (b) *v* forms.

EXPERIMENT 2: NAVIGATING TWO JOINED PATH SEGMENTS WITH SAME LENGTHS AND DIFFERENT WIDTHS

The purpose of this experiment was to observe the effects of a joint between two path segments on users' behaviors and model fitness. To increase internal validity, we simply connected two paths used in the experiment 1. This study was conducted directly after experiment 1 using the same apparatus and the same 13 participants.

Design and Procedure

The same values of A and W were used in this experiment; A (A_1 and A_2) = 480 and 640 pixels, and W (W_1 and W_2) = 15, 23, 33, and 45 pixels. A_1 and A_2 were always the same value, while W_1 and W_2 were always different values, which excludes the (relatively uninteresting) condition of a normal (equal width) steering task. The total combinations of the parameters were 2(A) × {4(W_1) × 4(W_2) – 4 (excluding W_1 = W_2)} = 24 conditions = 1 block. Participants first performed half a block (12 trials) in random order as a practice session, and then performed five blocks of actual trials. Movement direction was always to the right. The recorded data for the actual tasks were 24 conditions × 5 blocks × 13 participants = 1560 trials. The total time taken was 15 or 20 minutes. Two paths were connected at their centers on the y-axis as illustrated in Figure 1c, and the path segment joint was always located at the center of the display.

Results

After omitting lifting-pen instances (22 trials), the total number of trials was 1703, with 143 errors (8.40%). Below, we first analyze model fitness and present analyses of *MT* and error rates later.

Model Fitting

At first, we check whether the steering law holds for each of the two path segments (path1 and path2) separately. We then check whether the simple sum of two *ID*s (ID_{2SS}, Equation 9) model user performance for the entire path well.

With six data points, Figure 6a shows that the steering law held well for narrowing path sequences (i.e., W_1 > W_2). Figure 6b shows that the *widening* condition follows the law too. The fit without separating tunnel type (*narrowing* or *widening*) is not as good (R^2 > 0.91, Figure 6c). Thus, our hypothesis for a need to create a steering law for joined path segments is not strongly supported for the tested configurations. Figure 7a-c show the results of path2, and Figure 8a-c show the model fitness using the ID_{2SS} model.

Note that, the "*no separation*" graphs in Figure 6c, Figure 7c, and Figure 8c did not merge *MT* data with the same *ID* values. For example, in path1 (Figure 6), the times on *ID* = 19.4 bits were 1295 and 1037 ms for (a) *narrowing* and (b) *widening* respectively. If we use one merged point for *narrowing* and *widening* conditions on the same *ID* value, the *MT* for *no separation* is 1209 ms. The merged data is not the average of the two tunnel types, due to the different number of data points. The results for *no separation* using merged *MT* on the same *ID* are as follows:

Path1 time $MT = +294.2 + 45.92 \times ID$, with $R^2 = 0.981$

Path2 time $MT = -17.94 + 46.94 \times ID$, with $R^2 = 0.992$

Total time $MT = -137.3 + 55.51 \times ID$, with $R^2 = 0.995$

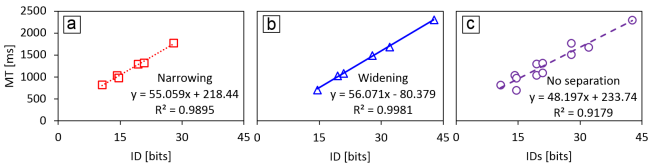

Figure 6. Model fitness of path1 in conditions of (a) narrowing, (b) widening, and (c) no separation of tunnel types.

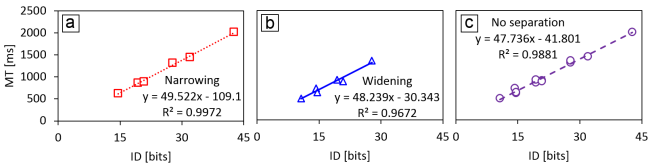

Figure 7. Model fitness of path2 in each condition.

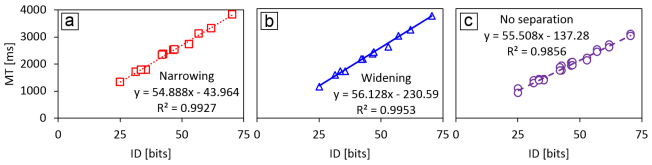

Figure 8. Model fitness of total times for each condition.

Movement Time MT

Because of the combinations of tunnel parameters, we cannot use an ANOVA with A, W_1, and W_2 as independent variables. For example, a condition of W_1 = 15 does not have W_2 = 15. In addition, (path1 × *narrowing*) and (path2 × *narrowing*) have different *ID* values (see Figure 6a and Figure 7a), and thus an ANOVA for separating path1 and path2 cannot use *ID* values as an independent variable. Therefore, we analyze only the total time using *tunnel type* (*narrowing* or *widening*) and ID_{2SS} as independent variables.

We observed main effects for *tunnel type* ($F_{1, 12} = 15.405$, $p < .01$) and *ID* ($F_{11, 132} = 41.969$, $p < .001$). The post hoc test shows that navigation for *narrowing* requires longer times, 2456 ms, compare to *widening,* 2326 ms ($p < .01$). The time required tends to grow with larger *ID* values.

Errors

We observed main effects for *tunnel type* ($F_{1, 12} = 9.302$, $p < .05$) and *ID* ($F_{11, 132} = 6.156$, $p < .001$). The post hoc test shows that the error rate for *narrowing*, 54/834 = 6.47%, is less than for *widening*, 89/869 = 10.2% ($p < .05$). The error rate tends to increase with larger *ID* values.

Discussion with Speed Profile Analysis

As shown in Figure 6-8, the steering law held reasonably well for all conditions in experiment 2. Hence, we wanted to analyze if users' strategies had not changed compared to those in experiment 1. To verify this question, we analyze the speed profiles for experiments 1 and 2 together.

A red line in Figure 9a shows the average speed profile on the x-axis for all participants under the condition of A = 480, W_1 = 23, and W_2 = 15 pixels in experiment 2. Because the raw data at the 8 ms sampling rate were very noisy and because we want to focus on the path segment joint, we re-sampled the cursor trajectories at every 40 pixels on the x-axis. The time for path1 (W_1 = 23) was 1323 ms, and for path2 (W_2 = 15) was 1444 ms. The two blue lines in Figure 9a show speeds in experiment 1 with the same width as path1 and path2 of experiment 2. The average times were 911 ms for W = 23 and 1451 ms for W = 15. The times for path2 in experiment 2 had only a small difference from the corresponding tasks in experiment 1 (7 ms, 0.77% longer), while the same correspondence in path1 shows a marked difference (412 ms, 45% longer).

A red line in Figure 9b shows the speed for the *widening* condition of A = 480, W_1 = 15, and W_2 = 23 pixels. Similar to the *narrowing* condition, the time for path1 of 1688 ms was significantly longer than that of experiment 1 (237 ms, 16% longer), while path2 with 890 ms was less than in experiment 1 (21 ms, 2.3% shorter).

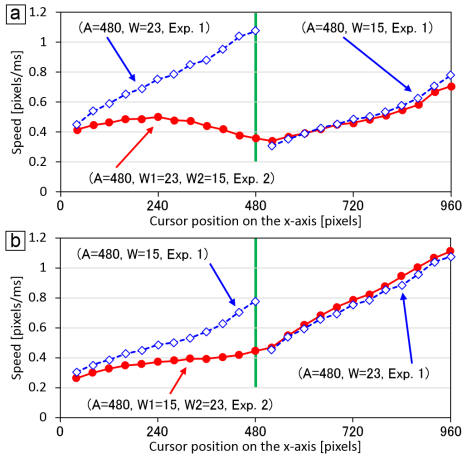

Figure 9. Red lines show the average speed profiles under the condition of A = 480, W = 23 and 15 for (a) *narrowing* and (b) *widening* path segments in experiment 2. Blue lines show the data from experiment 1. The green line at the center is the path joint. The speed at the start line is undefined.

At the start point of a path, it is natural that the speeds are slower than the top-speed for both *narrowing* and *widening*, because many users touched the surface with the stylus just before the start line and then gradually increased the speed. However, the speed at the first plot point in experiment 2 is slower than the speed at the start of experiment 1. This means that users anticipated the following path and they tried to limit their top speed at or even before the start. In addition, users changed their steering behaviors in the first path segment (path1) in the presence of a second path segment. Although the speed gradually increased until the end in experiment 1 (blue lines), in experiment 2 the speed began to decrease at x = 240 (the center of path1) for *narrowing* conditions. Furthermore, the top speed did not reach the same speed for a path with a width of 23 pixels compared to the speed of experiment 1. To be specific, users decreased the speed at around 0.36 pixels/ms before

the joint as shown in Figure 9a. In the second path segment, they easily reached and then exceeded that speed. Thus, we speculate that users decreased their speed *more than necessary* in path1 in the presence of a second path segment.

Why did the users significantly reduce their speed in the presence of a subsequent path segment? Here, we explain these behaviors through referring to work outside of HCI, namely several studies of similar conditions in the psychophysics field: When a person walks on a path and has to pass through a gate, s/he rotate the shoulders if the gate width is less than 1.3 × shoulder width [29]. Obviously, there is no concern of hitting the gate for such a gate width, even if subtle movements of the body during walking are considered, but we still naturally rotate the body. Humans anticipate and prepare more than necessary in advance in order to avoid an accident. We fundamentally want to avoid errors and put in effort, even if the effort may be wasted later. Higuchi et al. performed another study on gate passing [14] where participants answered that they could pass through the gate at 2.8 m in front of the gate. They predicted that they could not pass through the gate if the width was less than 1.15 × shoulder width. Hence, they could not perfectly predict the gate width, and if that width would require shoulder rotation.

In summary, humans change their actual behavior to avoid errors, and the necessity of the behavior change is partially determined in advance. In our experiment 2, the excess speed reduction for the *narrowing* condition might occur to avoid going over the boundaries when entering path2. The long distance of the deceleration in advance of the segment joint can also be explained through the analogy with Higuchi et al.'s study; users reliably anticipate and determine whether they should change their later behavior (i.e., reduce their speed).

For other tunnel parameters not shown in Figure 9 we observed similar tendencies; speeds in path2 are close to the results of experiment 1; those in path1 for *narrowing* follow an inverted "U" shape; and speeds in path1 for *widening* gradually increase, but slower than for experiment 1.

Although users exhibited significantly different behaviors, the steering law still held for any conditions in experiment 2. Hence our results demonstrate an aspect of generality of the steering law: we can accurately predict the total time for the two joined two path segments.

However, this still poses additional questions. First, does the steering law fit hold for conditions with different path segment lengths, i.e., $A_1 \neq A_2$? Experiment 2 included only conditions with $A_1 = A_2$ because our purpose was to analyze the effects of the path segment joint in isolation. The simple sum of two *ID* values was sufficient to model the total performance for $A_1 = A_2$ conditions, but this might only hold if the weights of two *ID* values are equivalent. If the balance is broken, for example, $A_1 = 100$ and $A_2 = 400$ pixels, some appropriate weights could be needed, such as:

$$\frac{A_1}{A_1 + A_2} \times ID_1 + \frac{A_2}{A_1 + A_2} \times ID_2 \quad (13)$$

or,

$$A_1 \times ID_1 + A_2 \times ID_2 \quad (14)$$

Another question is if the steering law ID_{2SS} model applies for conditions with $W_1 = W_2$? Such conditions were omitted in experiment 2 to test only paths with a joint. If the results of constant-width path differ from those with a joint, we have to predict times with a separate model. To analyze the generality of the steering law for such conditions, we conducted another experiment.

EXPERIMENT 3: NAVIGATING TWO JOINED PATH SEGMENTS, INCLUDING CASES WHERE LENGTHS ARE DIFFERENT AND WIDTHS ARE EQUAL

The purpose of this experiment was to validate the applicability of the steering law for two joined path segments, including cases where lengths are different and widths are equal (i.e., one linear path). The same 13 participants joined, and the same apparatuses were used. Depending on each participant this study was conducted 12 to 20 days after experiment 1 and 2.

Design and Procedure

Figure 10 shows the path parameters in this experiment. Five A_1 values (150, 250, 400, 600, and 800 pixels, or 35.0, 58.3, 93.2, 140, and 186 mm respectively) and three W values for both W_1 and W_2 (15, 23, and 39 pixels, or 3.50, 5.36, and 9.09 mm respectively) were tested. A_2 was always 400 pixels. Thus, the ratio of A_1/A_2 was 0.375, 0.625, 1.00, 1.50, and 2.00, respectively. In this experiment we included conditions with the same values of W_1 and W_2. The total combinations of the parameters were $5(A_1) \times 1(A_2) \times 3(W_1) \times 3(W_2) = 45$ conditions = 1 block. Participants first performed 20 trials from these 45 conditions in random order as a practice session, and then performed four blocks as actual trials. Movement direction was always to the right. The recorded data for the actual tasks were 45 conditions × 4 blocks × 13 participants = 2340 trials. The total time taken was 20 or 25 minutes. The condition of *tunnel type* (*narrowing*, *widening*, and *constant*) was defined by the combination of W_1 and W_2. The two paths were joined at the centers on the y-axis, and the path joint always located at the center of the display.

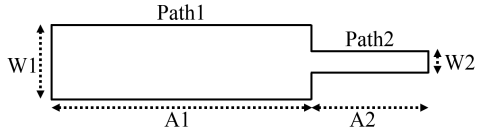

Figure 10. Parameter definition for experiment 3 with two joined path segments with unequal length. This image illustrates a condition with $A_1 > A_2$, and $W_1 > W_2$.

Results

After omitting lifting-pen instances (3 trials), the total number of trials was 2582, with 242 steering errors (9.37%). We cannot analyze the data using ID_{2SS} as an independent

variable because the three *tunnel types* had different *ID*s. Hence, we compare *MT* and error rates using only *tunnel types*.

Movement Time MT

We observed a main effect of *tunnel type* ($F_{2, 24} = 10.950$, $p < .001$). The average *MT* was 1735, 1643, and 1551 ms for *narrowing*, *widening*, and *constant* respectively. The post hoc test shows that navigation for *narrowing* requires longer times than constant ($p < .01$). The other pairs show no significant difference.

Errors

We observed no main effect of *tunnel type* ($F_{1, 12} = 0.057$, $p = .945$). The results were 81/861 = 9.41% for *narrowing*, 79/859 = 9.20% for *widening*, 82/862 = 9.51% for *constant*.

Model Fitting

Figure 11a-c show that steering law held using 15 data points for each *tunnel type* ($R^2 > 0.95$), and Figure 11d shows a good fit using all 45 data points ($R^2 > 0.96$).

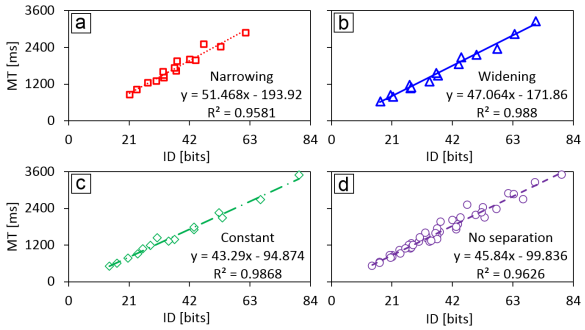

Figure 11. Model fitness in conditions of (a) *narrowing*, (b) *widening*, (c) *constant*, and (d) *no separation*.

Discussion with Speed Profile Analysis

Figure 12 shows the average speed profiles. We re-sampled at every 50 pixels as a common divisor of the five A_1 values, after confirming 25 pixels still showed noisy lines.

Figure 12a shows that users could not accelerate in the first path segment (path1) due to the extremely short distance. Also, the speed in path1 seems to adjust to an appropriate value to enter path2. This can be also confirmed by comparing to Figure 12e; the maximum speed in $A_1 = 800$ was 0.620 pixels/ms, while that in $A_1 = 150$ was 0.477 pixels/ms (23% slower). This means that the users cannot accelerate the cursor before the path ends, if A_1 is too short. Senanayake et al. [25] and Thibbotuwawa et al. [28] observed similar behaviors for a single linear path.

In joined path segments, the speed could not reach the appropriate value in the first segment, while the speed in the second one reached the appropriate value for W_2. Thus, users' performance seemed not to follow the steering law predicted by Equation 12. This breaks the consistency between path1 and path2. Furthermore, the average speed in path1 for *narrowing* condition differed strongly depending on the value of A_1. The speeds in path1 calculated via $A_1/(MT$ for path1) were 0.360, 0.393, 0.422, 0.432, 0.432 pixels/ms for A_1 = 150 to 800 pixels, respectively. The speed reached a constant value around A_1 = 400 or 600 pixels. On the other hand, for *widening* conditions, the speeds were 0.341, 0.358, 0.323, 0.338, 0.308 pixels/ms in path1 of W_1 = 15, which show no clear tendency of acceleration/deceleration with increasing A_1.

For the *constant* condition, as expected, the speeds generally increased like the results of experiment 1. In summary, clear differences are caused by the conditions of *tunnel type*, path length, and path width. Still, the steering law showed excellent fits for any situations in experiment 3. Therefore, we confirmed an aspect of generality of the steering law; in two joined linear path segments, the steering law holds regardless of the differences of path length and width, including equivalent lengths and widths.

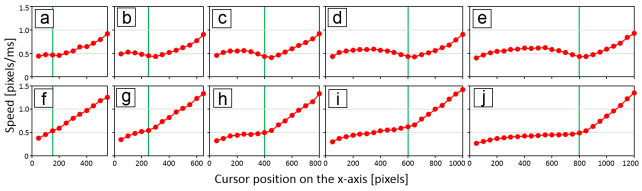

Figure 12. Average speed profiles under the condition of W = 23 and 15 for (top) *narrowing* and (bottom) *widening* conditions. (left to right) A_1 = 150 to 800 pixels respectively. Green lines at the center show the path joint.

OVERALL DISCUSSION

Auto-weight Function in Steering Law Structure

According to the results of experiments 2 and 3, the steering law ID_{2SS} held for two joined linear path segments. For a range of 0.375 to 2.00 for A_1/A_2, the robustness of the law was confirmed through accurate model fits. We speculated initially that the balance of ID_1 and ID_2 would break if the path lengths were different, but this hypothesis was not supported. Again, summing the two *ID*s means $ID_{2SS} = A_1/W_1 + A_2/W_2$. We consider that the structure of this sum itself has weights. For example, in a condition of A_1 = 800 and A_2 = 400 pixels, weights of 2:1 might be required. However, the ID_{2SS} model of $800/W_1 + 400/W_2$ already has appropriate weights through the two A factors. In hindsight, this "auto-weighting" function is inevitable due to the structure of the steering law. Yet this function had not been documented in the literature, likely because steering tasks with joined path segments have been not analyzed in detail.

Anticipation of the Following Path

Our hypothesis of that users change their behaviors affected by a path joint was strongly supported (Figure 9 and 12). Users determined the need to accelerate or decelerate by anticipating the following path segment being narrower/wider/equivalent compared to the current one.

Anticipation behaviors can be seen in the *narrowing* conditions more easily than the other ones. In a condition of W_1 = 23, W_2 = 15, and A_1 = 600 and 800 pixels in experiment 3, users began to decelerate about 250 pixels in advance of the joint (Figure 12d and e). Other parameter

combinations of W and A showed different peak points (Figure 12a, b, and c). Can we define this peak-to-joint distance as the *anticipation distance* for entering the second segment? Yet, we can even observe that users determined the strategy to enter path2 *before* entering path1. As shown in Figure 9, users' behaviors in path1 were significantly affected by the presence of path2 compared to without it. Therefore, *anticipation distance* is not an appropriate name for the distance of peak-to-joint, which we term D_{PJ}.

How is this D_{PJ} determined by users? According to Equation 12, D_{PJ} depends on the paths widths; the current speed is proportional to the current width, and the distance to decelerate increases as the difference between the appropriate speeds in path1 and path2 becomes greater. To confirm this, we reanalyze the data of experiment 2, which tested four W values. Figure 13 shows conditions with W_2 = 15 pixels. We assumed that the peak in path1 appears earlier as W_1 increases, but the results do not show a clear relationship between D_{PJ} and W_1. Although deriving a model for the relationship between them would pose an interesting contribution to the field of human performance modeling, none of models we derived fitted the actual data of experiments 2 and 3 well. One reason is that a sampling distance of 40 or 50 pixels is comparatively coarse for path widths of 15 to 45 pixels. A finer sampling could reveal the speed characteristics for each condition better, but when data is noisy (spiky) it is harder to define a true peak.

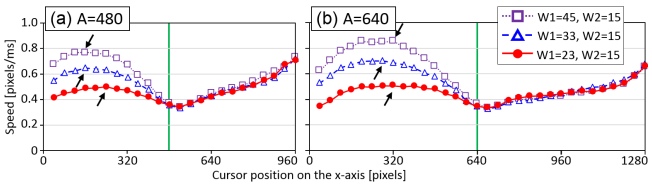

Figure 13. Average speed profiles of the *narrowing* condition in experiment 2. (a) A_1 = 480 and (b) A_2 = 640 pixels. Green lines show the path joint on the x-axis. Arrows indicate peaks in path1.

If A_1 is short, D_{PJ} has different characteristics. In the condition with W_1 = 23, W_2 = 15, and A_1 = 150 pixels, users had to set the speed for W_2 at the start (or even before the start) of path1, otherwise they would cause errors. Therefore, even if a model for D_{PJ} from path parameters is derived, the model could only adapt to conditions with sufficiently large values for A_1.

Although our experiments did not include a condition with various A_2 values, behaviors in path1 could also be affected by the value of A_2. Imagine an extreme condition: A_2 = 30 pixels for a *narrowing* condition. Here, users do not have to reduce the speed in path1 to pass through path2, and the task becomes close to a combination of a steering and a crossing [4] task.

Comparison with Other Models

The ID_{2SS} model accurately modeled steering through two joined paths segments. However, according to the speed profiles, user behaviors in joined paths were different from those in a single segment. Thus, we explore a model which reflects human behavior better than a sum of two ID values.

Weighted Models

The fitness of the weighted models are as follows: for experiment 2, R^2 = 0.986 and 0.908 (Equation 13 and 14, respectively), and for experiment 3, R^2 = 0.913 and 0.910. We assume that the reason behind the reduced fitness is that these models do not consider the user behaviors shown in Figure 9. Therefore, more sophisticated models are required to explain the users' behaviors.

Deriving Better Models for Users' Behaviors

Predictive model fitness cannot be discussed only through comparing R^2 values, because a complex model with many free parameters naturally increases the fit. Hence, we also compare with the Akaike information criterion (AIC) [6]. This statistics method balances the complexity of the model (i.e., number of free parameters) and the fitness, and determines the comparatively best model. As a brief explanation, a model with (a) lower AIC value is a better one, (b) $AIC \leq (AIC_{\text{minimum}} + 2)$ considers comparisons with better models, and (c) $AIC \geq (AIC_{\text{minimum}} + 10)$ is safely rejected. This analysis method was also used for selecting a pointing task model by Ren et al. [22] and Chapuis and Dragiceivc [8].

Another alternative candidate model is to use three free parameters for two steering IDs, similar to Dennerlein [9]:

$$ID_{3SS} \text{ model: } MT = a + b\left(\frac{A_1}{W_1}\right) + c\left(\frac{A_2}{W_2}\right)$$

and we call this the ID_{3SS} model. Next, we adapt Senanayake's model [24] to our experimental tasks. When a user navigates a single path, s/he can gradually accelerate and escape from the path (see blue lines in Figure 9). However, when s/he navigates two joined path segments, the speed in path1 cannot reach a speed comparable to that in a single path for both *narrowing* and *widening* conditions to correctly enter path2. Another way to state this is to say that a user reduces the speed to pass through the "gate" before entering the second segment. The preparation time to adjust the speed before entering the path2 is not modeled by the original steering law, and hence, the deceleration and longer times are unique characteristics of paths with joined segments. To take the time to enter the gate into account, it is reasonable to add a crossing time [4]. As illustrated in Figure 14, this motivates us to derive a model with three different performance phases. The core of this idea is that a user transits to a crossing operation for W_2 at a distance ($n \times W_1$) in advance of the joint (n is same as Senanayake's model). To cross a line of width W which lies at a distance A, we use the same formula as Fitts' law (Equation 3). Our new model for a combination of a steering, a crossing, and a steering task is:

$$MT = a + b\left(\frac{A_1 - nW_1}{W_1}\right) + c\log_2\left(\frac{nW_1}{W_2} + 1\right) + d\left(\frac{A_2}{W_2}\right)$$

	Model	*a*	*b*	*c*	*d*	R^2	*AIC*
Experiment 2	ID_{2SS}	-137.3 [-277.4, 2.883]	55.51 [52.54, 58.47]	—	—	0.986	290
	ID_{3SS}	-137.3 [-243.0, -31.51]	51.77 [48.88, 54.67]	59.24 [56.35, 62.13]	—	0.992	277
	ID_{4SCS}	-319.0 [-674.8, 36.90]	60.99 [53.32, 68.66]	187.5 [40.37, 334.7]	49.73 [41.85, 57.62]	0.994	272
	ID_{3SCS}	-67.71 [-189.0, 53.61]	55.45 [53.41, 57.48]	80.02 [47.30, 112.7]	—	0.996	272
Experiment 3	ID_{2SS}	-99.84 [-213.6, 13.92]	45.84 [43.06, 48.62]	—	—	0.963	578
	ID_{3SS}	-111.8 [-249.1, 25.46]	45.62 [42.48, 48.75]	46.75 [40.42, 53.08]	—	0.963	580
	ID_{4SCS}	-261.4 [-428.1, .94.70]	49.84 [47.03, 52.65]	228.3 [147.3, 309.3]	31.14 [23.82, 38.47]	0.979	556
	ID_{3SCS}	-115.1 [-295.1, 64.92]	45.97 [43.44, 48.49]	91.84 [33.66, 150.0]	—	0.970	571

Table 1. R^2 and *AIC* values for four candidate models. *a*, *b*, *c*, and *d* are constants with 95% CI values [min, max] in the models. Colored cells show the best values for each analysis method.

and we call this the ID_{4SCS} model. The difference from Senanayake's model is that a line to be crossed has no depth size *S*, as in pointing tasks. Another option is to add the two steering *ID* values as in the ID_{2SS} model:

$$MT = a + b\left(\frac{A_1 - nW_1}{W_1} + \frac{A_2}{W_2}\right) + c\log_2\left(\frac{nW_1}{W_2} + 1\right)$$

and we call this the ID_{3SCS} model.

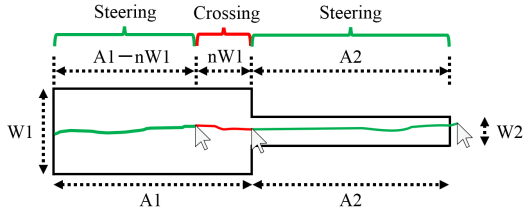

Figure 14. A model of two steering and one crossing phases.

As we explore models for the relationship between the total *MT* and path parameters, we analyze the composite of all data for experiments 2 and 3 (*no separation* conditions in Figure 8 and 11). Senanayake et al. showed that the fitness improved by changing the Fitts' *ID* model depending on target distances, and by changing the steering *ID* model when the *ID* was less than eight [24]. These alternatives were based on the fact that Fitts and steering *ID*s only depend on the distance *A* when *A* is small [13, 28]. However, for a fair comparison with the other models, we only use basic models of ID_{4SCS} and ID_{3SCS} models without changing the form of the *ID*. In our analysis, we fixed the *n* value to 5 as in previous work [24]. We observed that $(A_1 - nW_1)/W_1$ was sometimes negative in our ID_{4SCS} and ID_{3SCS} models, e.g., $A_1 = 150$, $W_1 = 39$, $n = 5$ results in –1.15. This can be explained by that users anticipated the joint even before the cursor entered path1. Because *n* was fixed, it was not counted as a free parameter in the *AIC* calculation.

Table 1 shows the result. Overall, the *SCS* models showed better fits than *SS* models. For *SS* models, 2*SS* showed a worse fit than 3*SS* for both R^2 and *AIC* values in experiment 2, and close fits in experiment 3. For *SCS* models, the difference in R^2 values was less than 1% in experiments 2 and 3. Yet, the *AIC* difference between 4*SCS* and 3*SCS* was more than 10 in experiment 3, with 4*SCS* being the better choice according to the *AIC* threshold criterion. In summary, although the *SS* models show good fits, taking the crossing operation between two steering operations into account provides even better predictions, with ID_{4SCS} being the best choice.

We also analyzed if the choice of $n = 5$ affected the outcome of our work. If we optimize *n* in the *SCS* models to maximize the R^2 value and to minimize the *AIC* value, their optimized values have little difference from those for $n = 5$. As these changes do not affect the overall conclusion on the model comparisons above, we conclude that the *SCS* models are not that sensitive to the *n* value, and this result justifies a previous study [24] which fixed the *n* value to 5.

Still, we initially believed that we could identify the true anticipation distance from the *n* value which optimizes the R^2 and *AIC* values. However, we found it quite difficult to clearly separate the steering and crossing phases, potentially because a steering operation can be interpreted as a sequence of crossing operations [1, 31]. Although determining the anticipation distance to pass through the gate is difficult, we conclude that adding a crossing term between two steering motions still improves model fitness.

While the *SCS* models explain the acceleration/deceleration behavior better, the difference in terms of *ID* between the *SS* and *SCS* models is small for experiment 2 and 3. Even when the crossing-*ID* was inserted, the replaced *ID* values were less than 3.5 bits, while experiment 3 explored *ID*s up to 80 bits. We assume that reason behind the small improvement of the model fitness comes from this small replacement of *ID* values.

Effects of Learning, Scaling, and Fatigue

In our study, user performance could be affected not only by *A* and *W*. For example, experiment 1 and 2 were performed first, and then experiment 3 was designed based on the results of these experiments. Thus, the order was not balanced, and learning effects could exist in our data

Another potential effect is scaling [3]. Experiment 1 involved (max) 149-mm lengths, which required mainly wrist movements with a forearm extension, while Experiment 3 included (max) 279.2-mm lengths, which can

require upper-arm movements. Such greater motor movements could degrade the steering performance [3].

Fatigue can also have an effect. It took seven minutes for experiment 1 and 25 min for experiment 3. For these reasons, the validity of direct data comparisons (e.g., for performance or speed) is somewhat limited in our study.

Application

Based on the speed profile, a support system could predict if a user wants to enter a narrow path. Thus, forward objects could be shrunk temporarily during lassoing when a user decelerates. Figure 15 shows the procedure; a) when a user decelerates to enter a narrow path during making a lasso stroke, b) the forward objects shrink to decrease steering difficulty. If the user would not like to enter the narrow path (e.g., the user just wants to stop there to finish the lasso), the shrinking effect does not have a negative effect on the operation. We will evaluate this idea in the future.

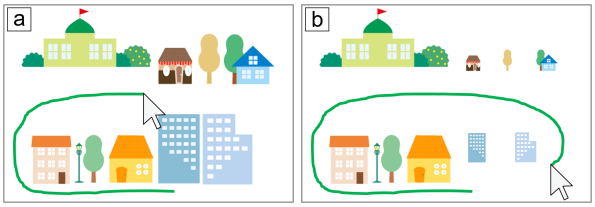

Figure 15. Facilitation system for lassoing tools. (a) When a user decelerates to enter the narrow path, (b) this system shrinks the objects in the (predicted) direction of the path.

Limitations and Future Work

The conditions tested in our experiments are still somewhat limited. Paths were only linear in shape and always connected at the center on the y-axis. Thus, the best strategy was moving the pen tip in the middle of the paths on the y-axis. If the two paths were connected at different positions, e.g., at the top as illustrated in Figure 16a, users' strategies would need to change. Here, some users might always navigate closely to the top boundary to reduce the total movement distance in the path like Figure 16a-(i). Others might navigate along the middle of path1, and then transit to the middle of path2 to avoid errors like Figure 16a-(ii).

The number of path segments is another limitation. We only tested two path segments with a single joint. In a condition where more paths are joined, different behaviors might be observed. As an extreme scenario, Figure 16b shows a sequentially connected repeated sequence of path1 (A_1, W_1) and path2 (A_2, W_2). Can we calculate the entire *ID* as (A_1/W_1 + A_2/W_2) × (number of path1 and path2), even if A_1 is short, e.g., 30 or 40 pixels? We assume that the entire *ID* becomes closer to the (entire length)/W_2 as A_1 becomes shorter, because the wider width of W_1 cannot be effectively used. Drewes presented this problem and made the same assumption [10]. Our experimental results support this hypothesis as follows: users have to avoid errors to accomplish steering tasks, and thus the speed in path1 must decrease to enter path2, based on the anticipatory behavior that we observed. If A_1 is short, because users anticipate the next path in advance of a joint, users have to continuously adjust the speed at the appropriate value for W_2, and thus the path width is expected to be always close to W_2. Further work is required to validate this hypothesis.

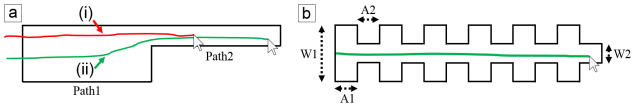

Figure 16. Two cases that our current work cannot describe adequately: (a) Steering through paths connected off-axis. (b) Steering through a sequence of six pairs of wide-to-narrow paths.

The four models derived in this paper accurately predict *MT* based on data for joined path segments. However, these models cannot predict *MT* for joined path segments from data for a single path, because slopes and intercepts of single and joined path segments are not similar (see Figure 5a and Table 1). To predict *MT* in joined path segments, we have to 1) measure *MT*s with various *ID*s in joined path segments, 2) regress the data (like Figure 11), and 3) use that to predict *MT* for a given *ID* value. We cannot predict *MT* from single path segment data, as the crossing-motion occurs only in joined path segments.

Our future work will also investigate a more general steering model that covers, e.g., linear, joined, and curved paths. In it, we might consider human-focused parameters, such as Higuchi et al.'s work on anticipation [14] and Zhou and Ren's work on subjective operational biases [34]. To achieve this goal, much more experimental work is needed.

CONCLUSION

We conducted several steering law experiments to investigate performance for steering tasks with two joined linear path segments. Users' behaviors significantly changed in the presence of a path joint, but a simple sum of two *ID*s for each path was enough to model the performance well. Four possible models were compared by the fitness using R^2 and *AIC*, and we identified model ID_{4SCS}, to be the best overall, as it takes account of the crossing operation required for entering the following path.

The speed profiles in joined path segments have not been studied before, nor have the speed differences from a single path segment and the reasons behind them been explored. Especially the deceleration data for narrowing conditions identifies fundamentally different behaviors relative to previous work. Our results thus provide a better understanding of steering motions, in particular for error avoidance strategies and anticipation of the successive path segment, which can be observed only in path sequences. In the future, we will investigate more complex conditions, including combinations of paths with changing widths and corners, towards a more general version of the steering law.

ACKNOWLEDGEMENTS

This work was supported by JSPS KAKENHI #15J11634. The first author also thanks his present affiliation, Yahoo Japan Corporation.

REFERENCES

1. Johnny Accot and Shumin Zhai. 1997. Beyond Fitts' law: models for trajectory-based HCI tasks. In *Proceedings of the SIGCHI Conference on Human Factors in Computing Systems* (CHI '97), 295–302. http://dx.doi.org/10.1145/258549.258760
2. Johnny Accot and Shumin Zhai. 1999. Performance evaluation of input devices in trajectory-based tasks: an application of the steering law. In *Proceedings of the SIGCHI Conference on Human Factors in Computing Systems* (CHI '99), 466–472. http://dx.doi.org/10.1145/302979.303133
3. Johnny Accot and Shumin Zhai. 2001. Scale effects in steering law tasks. In *Proceedings of the SIGCHI Conference on Human Factors in Computing Systems* (CHI '01), 1–8. http://dx.doi.org/10.1145/365024.365027
4. Johnny Accot and Shumin Zhai. 2002. More than dotting the i's --- foundations for crossing-based interfaces. In *Proceedings of the SIGCHI Conference on Human Factors in Computing Systems* (CHI '02), 73–80. http://dx.doi.org/10.1145/503376.503390
5. Scott Bateman, Andre Doucette, Robert Xiao, Carl Gutwin, Regan L. Mandryk, and Andy Cockburn. 2011. Effects of view, input device, and track width on video game driving. In *Proceedings of Graphics Interface* (GI '11), 207–214.
6. Kenneth P. Burnham and David R. Anderson. 1998. Model selection and multimodel inference: a practical information-theoretic approach. Springer. http://dx.doi.org/10.1002/sim.769
7. Géry Casiez, Patricia Plénacoste, and Christophe Chaillou. 2004. Does DOF separation on elastic devices improve user 3D steering task performance? In *Proceedings of the Asia Pacific Conference on Computer Human Interaction* (APCHI '04), 70–80. http://dx.doi.org/10.1007/978-3-540-27795-8_8
8. Olivier Chapuis and Pierre Dragicevic. 2011. Effects of motor scale, visual scale, and quantization on small target acquisition difficulty. *ACM Transactions on Computer-Human Interaction* (TOCHI), Vol.18, No.3, Article 13. http://dx.doi.org/10.1145/1993060.1993063
9. Jack Tigh Dennerlein, David B. Martin, and Christopher Hasser. 2000. Force-feedback improves performance for steering and combined steering-targeting tasks. In *Proceedings of the SIGCHI Conference on Human Factors in Computing Systems* (CHI '00), 423–429. http://dx.doi.org/10.1145/332040.332469
10. Heiko Drewes. 2013. A lecture on Fitts' law. http://www.cip.ifi.lmu.de/~drewes/science/fitts/A%20Lecture%20on%20Fitts%20Law.pdf
11. Colin G. Drury. 1971. Movements with lateral constraint. *Ergonomics*, Vo.14, No.2, 293–305. http://dx.doi.org/10.1080/00140137108931246
12. Paul M. Fitts. 1954. The information capacity of the human motor system in controlling the amplitude of movement. *Journal of Experimental Psychology*, Vol.47, No.6, 381–391. http://psycnet.apa.org/doi/10.1037/h0055392
13. Khai-Chung Gan and Errol R. Hoffmann. 1988. Geometrical conditions for ballistic and visually controlled movements. *Ergonomics*, Vol.31, No.5, 829–839. http://dx.doi.org/10.1080/00140138808966724
14. Takahiro Higuchi, Hajime Takada, Yoshifusa Matsuura, and Kuniyasu Imanaka. 2004. Visual estimation of spatial requirements for locomotion in novice wheelchair users. *Journal of Experimental Psychology: Applied*, Vol.10, No.1, 55–66. http://psycnet.apa.org/doi/10.1037/1076-898X.10.1.55
15. Errol R. Hoffmann. 1997. Movement time of right- and left-handers using their preferred and non-preferred hands. *International Journal of Industrial Ergonomics*, Vol.19, No.1, 49–57. http://dx.doi.org/10.1016/0169-8141(95)00092-5
16. Sergey Kulikov, I. Scott MacKenzie, and Wolfgang Stuerzlinger. 2005. Measuring the effective parameters of steering motions. In *Extended Abstracts of the SIGCHI Conference on Human Factors in Computing Systems* (CHI '05), 1569–1572. http://dx.doi.org/10.1145/1056808.1056968
17. Sergey Kulikov and Wolfgang Stuerzlinger. 2006. Targeted steering motions. In *Extended Abstracts of the SIGCHI Conference on Human Factors in Computing Systems* (CHI '06), 983–988. http://dx.doi.org/10.1145/1125451.1125640
18. Lei Liu, Jean-Bernard Martens, and Robert van Liere. 2011. Revisiting path steering for 3D manipulation tasks. *International Journal of Human-Computer Studies*, Vol.69, Issue 3, 170–181. http://dx.doi.org/10.1016/j.ijhcs.2010.11.006
19. Robert L. Pastel. 2006. Measuring the difficulty of steering through corners. In *Proceedings of the SIGCHI Conference on Human Factors in Computing Systems* (CHI '06), 1087–1096. http://dx.doi.org/10.1145/1124772.1124934
20. Nicolas Rashevsky. 1959. Mathematical biophysics of automobile driving. *Bulletin of Mathematical Biophysics*, Vol.21, No.4, 375–385. http://dx.doi.org/10.1007/BF02477896
21. Nicolas Rashevsky. 1970. Mathematical biophysics of automobile driving IV. *Bulletin of Mathematical Biophysics*, Vol.32, No.1, 71–78. http://dx.doi.org/10.1007/BF02476794

22. Xiangshi Ren, Jing Kong, and Xing-Qi Jiang. 2005. SH-model: a model based on both system and human effects for pointing task evaluation. *IPSJ Journal*, Vol.46, No.5, 1343–1353.
23. Xiangshi Ren and Xiaolei Zhou. 2011. An investigation of the usability of the stylus pen for various age groups on personal digital assistants. *Behaviour & Information Technology*, Vol.30, No.6, 709–726. http://dx.doi.org/10.1080/01449290903205437
24. Ransalu Senanayake, Errol R. Hoffmann, and Ravindra S. Goonetilleke. 2013. A model for combined targeting and tracking tasks in computer applications. *Experimental Brain Research*, Vol.231, No.3, 367–379. http://dx.doi.org/10.1007/s00221-013-3700-4
25. Ransalu Senanayake and Ravindra S. Goonetilleke. 2016. Pointing device performance in steering tasks. *Perceptual and Motor Skills*, Vol.122, No.3, 886–910. http://dx.doi.org/10.1177/0031512516649717
26. R. William Soukoreff, I. Scott MacKenzie. 2004. Towards a standard for pointing device evaluation, perspectives on 27 years of Fitts' law research in HCI. *International Journal of Human-Computer Studies*, Vol.61, No.6, 751–789. https://doi.org/10.1016/j.ijhcs.2004.09.001
27. Namal Thibbotuwawa, Ravindra S. Goonetilleke, and Errol R. Hoffmann. 2012. Constrained path tracking at varying angles in a mouse tracking task. *Human Factors*, Vol.54, No.1, 137–149. http://dx.doi.org/10.1177/0018720811424743
28. Namal Thibbotuwawa, Errol R. Hoffmann, and Ravindra S. Goonetilleke. 2012. Open-loop and feedback-controlled mouse cursor movements in linear paths. *Ergonomics*, Vol.55, No.4, 476–488. http://dx.doi.org/10.1080/00140139.2011.644587
29. William H. Warren Jr. and Suzanne Whang. 1987. Visual guidance of walking through apertures: body-scaled information for affordances. *Journal of Experimental Psychology: Human Perception and Performance*, Vol.13, No.3, 371–383. http://psycnet.apa.org/doi/10.1037/0096-1523.13.3.371
30. Shota Yamanaka and Homei Miyashita. 2016. Modeling the steering time difference between narrowing and widening tunnels. In *Proceedings of the SIGCHI Conference on Human Factors in Computing Systems* (CHI '16), 1846–1856. http://dx.doi.org/10.1145/2858036.2858037
31. Shumin Zhai, Johnny Accot, and Rogier Woltjer. 2004. Human action laws in electronic virtual worlds: an empirical study of path steering performance in VR. *Presence*, Vol.13, No.2, 113–127. http://dx.doi.org/10.1162/1054746041382393
32. Xiaolei Zhou, Xiangshi Ren, and Yue Hui. 2008. Effect of start position on human performance in steering tasks. In *Proceedings of the International Conference on Computer Science and Software Engineering* (CSSE '08), Vol.2, 1098–1101. http://dx.doi.org/10.1109/CSSE.2008.1310
33. Xiaolei Zhou, Xiang Cao, and Xiangshi Ren. 2009. Speed-accuracy tradeoff in trajectory-based tasks with temporal constraint. In *Proceedings of the IFIP International Conference on Human Computer Interaction* (INTERACT '09), 906–919. http://dx.doi.org/10.1007/978-3-642-03655-2_99
34. Xiaolei Zhou and Xiangshi Ren. 2010. An investigation of subjective operational biases in steering tasks evaluation. *Behaviour & Information Technology*, Vol.29, No.2, 126–135. http://dx.doi.org/10.1080/01449290701773701